Advances in Clinical Radiology 1 (2019) 193–214
ADVANCES IN CLINICAL RADIOLOGY

High-Resolution Magnetic Resonance Vessel Wall Imaging in Intracranial Atherosclerotic Disease

Ramez N. Abdalla, MD[a,b], Donald R. Cantrell, MD, PhD[a,c], Alireza Vali, PhD[a], Michael C. Hurley, MD[a,c], Ali Shaibani, MD[a,c], Timothy J. Carroll, PhD[d], Sameer A. Ansari, MD, PhD[a,c,e,*]

[a]Department of Radiology, Northwestern University, Feinberg School of Medicine, 676 North St. Clair Street, Suite 800, Chicago, IL 60611-2927, USA; [b]Department of Radiology, Ain Shams University, Cairo, Egypt; [c]Department of Neurological Surgery, Northwestern University, Feinberg School of Medicine, 676 North St. Clair Street, Suite 800, Chicago, IL 60611-2927, USA; [d]Department of Radiology, University of Chicago, 5841 S Maryland, Chicago, IL 60637, USA; [e]Department of Neurology, Northwestern University, Feinberg School of Medicine, 676 North St. Clair Street, Suite 800, Chicago, IL 60611-2927, USA

KEYWORDS
• HR MR VWI • BBMRI • ICAD • ICAS • T1 SPACE

KEY POINTS
- Overview on the epidemiology, risk factors, risk of recurrence and management of intracranial atherosclerotic disease.
- Description of vulnerable atherosclerotic plaques and stroke mechanisms in ICAD.
- Important points on how to perform and optimize HR MR VWI protocols.
- How to differentiate normal vessel from stable and unstable atherosclerotic plaques as well as other neurovascular pathology on MR VWI.
- Future advancements and limitations in MR VWI in ICAD.

INTRODUCTION

Although cervical carotid vessel wall imaging (VWI) is well established and now commonly used in clinical practice, the widespread adoption of intracranial VWI has been hindered by multiple technical challenges. Magnetic resonance (MR) VWI of the smaller and more tortuous intracranial anatomy requires higher spatial resolution and signal/noise ratio (SNR), while maintaining acceptable scan times to minimize motion-related artifacts. Although the optimal imaging protocols for intracranial VWI remain a topic of ongoing research, VWI is already clinically used in conjunction with conventional luminal imaging techniques in many leading medical centers to provide a more comprehensive assessment of intracranial atherosclerotic disease (ICAD) and vasculopathies.

This article highlights the epidemiology and risk factors contributing to intracranial atherosclerosis, the

Disclosures: None.

*Corresponding author. Department of Radiology, Northwestern University, Feinberg School of Medicine, 676 North St. Clair Street, Suite 800, Chicago, IL 60611-2927. *E-mail address:* s-ansari@northwestern.edu

https://doi.org/10.1016/j.yacr.2019.05.005
2589-8744/19/

histologic progression of ICAD, and the various mechanisms by which it can result in ischemic stroke. We will discuss the relevant technical factors that must be considered when optimizing MR VWI protocols. In addition, the MR VWI findings that may be related to ICAD plaque instability are described and differentiated from other intracranial vasculopathies. In addition, the current limitations and future directions of MR VWI in ICAD are discussed.

INTRACRANIAL ATHEROSCLEROTIC DISEASE EPIDEMIOLOGY AND RISK FACTORS

ICAD is the most common cause for stroke worldwide [1]. Stroke is the fifth leading cause of death, and it is the leading cause of disability in the United States, with an annual incidence of 795,000 cases, 87% of which are ischemic [2]. Among those, 8-17% are secondary to ICAD, with an annual risk of recurrence as high as 15% [3–6].

However, the risk of stroke caused by intracranial atherosclerosis varies greatly among different populations and ethnicities, ranging from 1% in non-Hispanic whites to 50% in Asian and Chinese populations [7]. In a population-based Rotterdam study of white Europeans, intracranial artery calcification was used as a surrogate marker for ICAD and was observed in 82% of the population, increasing with age from 10-30% in individuals 20 to 29 years old to 95% in those aged 80 years and older [8]. ICAD was observed significantly more in Asian, African, and Hispanic populations. In a study of the North American population in Manhattan, African American and Hispanic patients harbored 5 times higher rates of ICAD compared to whites, which corresponded with higher ischemic stroke rates amounting to 3, 13, and 15 per 1000 in whites, Hispanics, and African Americans, respectively [9]. In southern Asian and Chinese studies, ischemic strokes secondary to ICAD ranged from 33% to 54%, with one Chinese study identifying it as the underlying etiology for transient ischemic attacks (TIA) in 51% of patients [10–14]. The prevalence of asymptomatic ICAD detected on transcranial Doppler and MR angiography (MRA) studies had been reported in multiple studies to vary between 3.5% and 15% depending on age and ethnicity [7], with some Japanese and Chinese studies identifying asymptomatic ICAD rates as high as 15% and 20-30%, respectively [15,16]. One Chinese post mortem autopsy study reported that intracranial atherosclerosis was identified in at least 1 large intracranial artery in 30% of patients in their sixth and seventh decades and in 50% of patients in their eighth and ninth decades of life [17].

Multiple modifiable and nonmodifiable risk factors have been associated with ICAD, including age, gender, alcohol intake, smoking, hypertension, serum lipid profile, and diabetes [7,8,18]. Some studies have shown male gender to be a significant risk factor for asymptomatic ICAD [19], whereas others have found no association between male sex, smoking, or hyperlipidemia in asymptomatic disease [20]. Age, hypertension, and diabetes mellitus were found in several studies to be independent risk factors for symptomatic and asymptomatic ICAD [19–21]. Metabolic syndrome, which is a combination of risk factors (hypertension, hyperglycemia, hypercholesterolemia, hypertriglyceridemia, and increased abdominal fat related to insulin resistance) was shown to be highly prevalent in patients with ICAD, with some studies identifying it as an independent risk factor for symptomatic ICAD [22–24].

INTRACRANIAL ATHEROSCLEROTIC DISEASE STROKE RECURRENCE

Stroke progression and recurrence is common in ICAD-related ischemic events. Progressive neurologic deficits within 2 days of symptom onset have been reported in 14% of patients with ICAD [25]. Other studies have reported a 13% risk of symptomatic stroke recurrence within 2 to 7 days of the original event [26], and a 10% in-hospital mortality during the initial admission [27]. Another study showed that 56% of patients medically managed for ICAD-related infarcts were readmitted with recurrent ischemic stroke affecting the same arterial territory, with a median presentation time of 28 days from the initial event [28]. This same study also reported a 100% stroke recurrence in a 3-month period for patients with basilar artery stenosis [28]. In a long-term Chinese study of patients with ICAD stroke, the annual risk of stroke recurrence in the first year was 17.1% for patients with intracranial atherosclerosis alone and 24.3% for patients with combined intracranial and extracranial atherosclerotic disease [29]. Furthermore, one study showed that symptomatic recurrences represent only approximately 25% of the total recurrent strokes that can be documented on MRI [26]. In this study, 51% of patients developed new or recurrent ischemic strokes within 7 days as seen on MR diffusion-weighted imaging (DWI); however, only 13% of those infarcts were symptomatic [26]. Most of these recurrent strokes were noted in the same arterial territory, with the highest risk of

recurrence seen in women and patients presenting with greater than or equal to 70% stenosis [3].

INTRACRANIAL ATHEROSCLEROTIC DISEASE MANAGEMENT

Because patients with the greatest degree of atherosclerotic stenosis demonstrated the highest risk for recurrent stroke, initial interventional trials logically targeted ICAD lesions with early angioplasty and stenting to relieve luminal narrowing in the hope that this would decrease the risk for stroke progression or recurrence. This approach was further encouraged by the favorable outcomes of cervical carotid interventions in the NASCET (North American Symptomatic Carotid Endarterectomy Trial) and CREST (Carotid Revascularization Endarterectomy vs. Stenting Trial) trials [30,31]. However, early data quickly refuted this hypothesis. In 2011, the SAMMPRIS (Stenting and Aggressive Medical Management for Preventing Recurrent Stroke in Intracranial Stenosis) randomized control trial comparing endovascular angioplasty/stenting with aggressive medical management in patients with severe stenosis (>70%) was terminated after an interim analysis showed the superiority of medical management with lower rates of recurrent strokes within 30 days (5.8% vs 14.7%) as well as no long-term benefit at 1 year (12% vs 20%) [32]. These results were reproduced by the VISSIT (Vitesse Intracranial Stent Study for Ischemic Stroke Therapy) trial that same year, which compared endovascular intervention using balloon-expandable stents with medical management in symptomatic (>70%) intracranial stenosis and showed that the 1-year risk for stroke recurrence was significantly higher with stenting compared with the medical management group (36.2% vs 15.1%) [33]. Table 1 summarizes the results of the largest randomized trials and data registries comparing different treatments for ICAD. Given the results of these randomized controlled trials, maximal medical management remains the mainstay of clinical practice in patients with stroke secondary to ICAD.

However, many patients fail medical management, returning with recurrent ischemic events, and expert opinion maintains that properly selected patients may still benefit from endovascular treatment in refractory ICAD. To this date, no randomized controlled trials have been conducted comparing the safety and efficacy of endovascular treatment versus medical management in patients presenting with recurrent strokes despite aggressive medical therapy, but many practitioners and institutions think it is reasonable to pursue endovascular treatment in these cases. The early identification of patients at risk for failing aggressive medical management as per the SAMMPRIS criteria is a goal of current research, because these patients may benefit from aggressive endovascular interventions. The proper selection of these patients requires a better understanding of the underlying histopathology of ICAD plaques and the mechanisms of stroke resulting from different plaque subtypes.

LUMINAL ANGIOGRAPHY LIMITATIONS

The diagnosis and characterization of intracranial atherosclerosis have traditionally been limited to luminal imaging techniques that evaluate the degree of intracranial stenosis. Digital subtraction angiography (DSA) is the gold-standard luminal imaging technique, and it can accurately depict stenoses in both large, proximal vessels as well as small, distal arteries, but its invasive nature carries a small risk of TIA/stroke itself. Noninvasive luminal imaging modalities include computed tomography angiography (CTA) and MR angiography (MRA), which are widely accessible, safe, and can accurately diagnose stenoses in proximal, intracranial arteries. However, the evaluation of smaller, more distal intracranial vessels with CTA and MRA is limited [40,41].

DSA, CTA, and MRA imaging techniques are inherently limited to evaluation of the vessel lumen, resulting in the underdiagnosis of ICAD because clinically significant disease may result in outward remodeling of the affected vessel without stenosis [42,43]. As initially described in the coronary arteries, intracranial atherosclerotic plaques first expand outward before causing luminal narrowing [44,45], and thus nonstenotic plaques are underestimated or missed on luminal imaging techniques [46–48]. For example, in a postmortem study of 339 patients with stroke, 59% harbored intracranial plaques, whereas only 37.2% of these plaques were associated with a stenosis greater than 30%, suggesting that nonstenotic plaques comprise the majority of ICAD [49]. Other studies have even reported that ICAD plaques with positive remodeling (outward wall growth) are more likely to be symptomatic and pose a higher risk for downstream microemboli compared with atherosclerotic disease with negative remodeling (vessel luminal narrowing) [43,50]. For this reason, luminal imaging techniques alone cannot accurately identify high-risk atherosclerotic lesions. In addition, luminal imaging is often unable to differentiate ICAD from the similar-appearing multifocal stenoses of alternative intracranial vasculopathies [51–53].

TABLE 1
Randomized Controlled Trials and Data Registries Comparing the Effects of Different Treatments On Stroke Recurrence in Patients with Intracranial Atherosclerotic Disease

Study/Date	Patients	Time from Symptom Onset	Arterial Disorder	Treatment Group	Control Group	Duration of Follow-up	Primary Outcome	Cases vs Controls (%)	Risk Reduction/OR
WASID, Chimowitz et al, [34], 2005	569	90 d (median, 16 d)	50%–99% stenosis	Warfarin (target INR 2.0–3.0; n = 289)	Aspirin (1300 mg/d; n = 280)	1.8 y (mean)	Ischemic stroke, brain hemorrhage, death from vascular cause	21.8 vs 22.1	No difference (HR, 1.04; 95% CI, 0.73–1.548; P = .83) with warfarin
ESPRIT, Halkes et al [35], 2006	2739	6 mo	Presumed arterial origin (degree of stenosis not specified)	Aspirin 30–325 mg (median, 75 mg) daily plus dipyridamole (200 mg twice daily); n = 1363	Aspirin 30–325 mg (median, 75 mg) daily; n = 1376	3.5 y (mean)	Death from vascular cause, nonfatal stroke or MI, major bleeding	13 vs 16	Risk reduction (HR, 0.80; 95% CI, 0.66–0.98; ARR 1.0% per year; 95% CI, 0.1–1.8) with aspirin plus dipyridamole
ESPRIT, Halkes et al [36], 2007	1068	6 mo	Presumed arterial origin (degree of stenosis not specified)	Oral anticoagulant (target INR, 2.0–3.0; n = 536)	Aspirin 30–325 mg (median, 30 mg) daily; n = 1376	4.6 y (mean)	Death from vascular cause, nonfatal stroke or MI, major bleeding	19 vs 18	No difference (HR, 1.02; 95% CI, 0.77–1.35) with oral anticoagulation
FISS, Wong et al [37], 2007	353	48 h	Large artery occlusion (300 only intracranial, 42 had both intracranial and extracranial and 11 only extracranial)	LMWH (subcutaneous nadroparin calcium 3800 anti–factor Xa IU/0.4 mL) twice daily for 10 d followed by aspirin 80–300 mg once daily for 6 mo; n = 180	Aspirin 160 mg daily for 10 d followed by aspirin 80–300 mg once daily for 6 mo; n = 173	6 mo	Good outcome (Barthel index $\geq$ 85)	73 vs 69	ARR, 4%; 95% CI, −5 to 13 with aspirin
PRoFESS, Sacco et al [38], 2008	20,332	90 d	28% of patients had large artery atherosclerosis	Aspirin 25 mg plus 200 mg of extended-release dipyridamole twice daily; n = 10,181	Clopidogrel 75 mg daily; n = 10,151	2.5 y (mean)	Recurrent stroke	9 vs 8.8	No difference (HR, 1.01; 95% CI, 0.92–1.11) with aspirin and extended-release dipyridamole

TOSS-2 [39], 2011	457	2 wk	Focal stenosis (mild, moderate, or severe) and occlusion (~1% of cases) in MCA or BA	Cilostazol 100 mg twice daily plus aspirin 75–150 mg once daily; n = 232	Clopidogrel 75 mg once daily plus aspirin 75–150 mg once daily; n = 225	7 mo	Progression of stenosis on MRI	9.3 vs 15.5	No difference (OR, 0.61; $P = .092$) with cilostazol plus aspirin
SAMMPRIS, Chimowitz et al [32], 2011	451	30 d (median, 7 d)	70%–99% stenosis	PTAS using the Wingspan stent plus AMM (clopidogrel 75 mg daily plus aspirin 325 mg daily followed by aspirin monotherapy with controlling SBP<140 mm Hg (and <130 mm Hg in diabetics) and LDL<70 mg/dL using statin with lifestyle modification); n = 227	AMM (clopidogrel 75 mg daily plus aspirin 325 mg daily followed by aspirin monotherapy with controlling SBP<140 mm Hg (<130 mm Hg in diabetics) and LDL<70 mg/dL using statin with lifestyle modification); n = 224	1 y	Stroke or death within 30 d of enrollment or after revascularization procedure of qualifying lesion Stroke in qualifying artery territory beyond 30 d	20 vs 12.2	AMM is superior ($P = .009$) to PTAS plus AMM in patients with severe symptomatic intracranial stenosis
VISSIT, Zaidat et al [33], 2015	112	30 d	70%–99% stenosis	Balloon-expandable stent plus medical management (clopidogrel 75 mg daily plus aspirin 81–325 mg daily for 3 mo followed by aspirin monotherapy); n = 59	MM (clopidogrel 75 mg daily plus aspirin 81–325 mg daily for 3 mo followed by aspirin monotherapy); n = 53	1 y	Stroke in the same vascular territory within 12 mo TIA in the same vascular territory 2–12 mo	36.2 vs 15.1	MM is superior ($P = .02$) to balloon-expandable stent plus MM in patients with severe symptomatic intracranial stenosis

Abbreviations: ARR, absolute risk reduction; AMM, aggressive medical management; BA, basilar artery; CI, confidence interval; ESPRIT, European/Australasian Stroke Prevention in Reversible Ischaemia Trial; FISS, Fraxiparine in Ischaemic Stroke; HR, hazard ratio; INR, international normalized ratio; LDL, low-density lipoprotein; LMWH, low-molecular-weight heparin; MCA, middle cerebral artery; MI, myocardial infarction; OR, odds ratio; PRoFESS, Prevention Regimen for Effectively Avoiding Second Strokes trial; PTAS, percutaneous transluminal angioplasty and stenting; SAMMPRIS, Stenting and Aggressive Medical Management for Preventing Recurrent Stroke in Intracranial Stenosis; SBP, systolic blood pressure; TOSS-2, Trial of cilOstazol for Symptomatic intracranial Stenosis 2; TIA, transient ischemic attack; VISSIT, Vitesse Intracranial Stent Study for Ischemic Stroke Therapy; WASID, Warfarin-Aspirin Symptomatic Intracranial Disease.

Intracranial MR VWI has recently been developed and optimized to augment traditional luminal imaging techniques. Proper clinical application of VWI allows the detection of nonstenotic inflammatory atherosclerotic plaques and may help to differentiate between ICAD and alternative intracranial vascular diseases [54–58].

INTRACRANIAL ATHEROSCLEROTIC DISEASE AND VULNERABLE PLAQUE PATHOPHYSIOLOGY

Intracranial atherosclerosis typically develops initially in the fourth decade of life, approximately 2 to 3 decades later than atherosclerosis of the coronary arteries and extracranial carotid arteries [59]. However, some studies have reported an earlier onset of ICAD in Asian patients compared with Caucasians [60]. The basilar artery (BA) followed by the proximal middle cerebral artery (MCA) are the sites most commonly affected by ICAD [59,61].

The severity of coronary atherosclerotic disease has been shown to correlate with the severity of extracranial carotid atherosclerosis within the same patient, but there is a weaker correlation with the severity of ICAD [62]. This finding may be explained by the histologic differences between intracranial arteries and extracranial carotid or coronary arteries. Although they share the same 3 vessel wall layers (inner intima, middle media, and outer adventitia), intracranial arteries possess a thicker fenestrated internal elastic lamina and a thinner media and adventitia. In contrast with extracranial arteries, intracranial arteries possess no external elastic lamina or vasa vasorum, rather facilitating exchange with the cerebral spinal fluid [63].

Atherosclerosis was initially described as an inside-out process, beginning with irritation to the intima caused by chronic endothelial disruption from long-term exposure to vascular risk factors. However, recent hypotheses suggest that atherosclerotic plaques may instead develop in an outside-in manner, beginning in the adventitia [64]. The vasa vasorum is a network of microvessels present in the adventitia that supplies oxygen and nourishment to the arterial wall, and has been implicated in the development, progression, and destabilization of atherosclerotic plaques. It has been postulated that the vasa vasorum contributes to plaque deposition and progression by carrying inflammatory cells into the plaque and to plaque destabilization by rupturing to cause intraplaque hemorrhage [65–67]. Intracranial arteries possess thinner media and adventitial layers and lack the external elastic lamina, which renders them more permeable to nutrients and oxygen diffusion from the nutrient-rich cerebrospinal fluid (CSF) bathing those arteries. The availability of oxygen and nutrients from the surrounding CSF removes the need for a vasa vasorum to deliver nutrients to the intracranial arteries. However, the development of atherosclerosis later in life may render the intracranial arteries less permeable to nutrients from the CSF, and it has been suggested that the vasa vasorum proliferates as a result of this decreased permeability to provide the arterial wall with the necessary nutrients [56,68]. Data shows that the vasa vasorum is normally present in the extracranial arteries and only the most proximal intracranial arteries, but it extends contiguously into the more distal intracranial arteries with aging, vessel wall thickening, and hypoxia in order to meet the increasing nutrient demands [56,69]. The distribution of intracranial vasa vasorum may explain the observation that atherosclerosis most commonly affects the proximal intracranial arteries.

Plaque formation advances through a 3-stage process. First, in the fatty-streak stage, low-density lipoprotein (LDL) accumulates in the intima and oxidizes into oxidized LDL (OxLDL), which subsequently activates endothelial cells to produce cytokines and express adhesion proteins. Adhesion proteins allow T lymphocytes and monocytes to infiltrate the endothelium, and these cells later differentiate into macrophages and engulf OxLDL, ultimately forming foam cells that accumulate on the arterial wall and create the characteristic lipid streaks. In the second stage, the fibrous-plaque stage, macrophages and T lymphocytes secrete cytokines and growth factors (interleukin-1 and tumor necrosis factor), thereby initiating a chronic inflammatory process, with resultant proliferation and migration of smooth muscles cells (SMCs) from media to intima, where they engulf OxLDL to form SMC-derived foam cells. These SMC-derived foam cells then release extracellular matrix proteins that form the fibrous cap which covers the plaque and characterizes this stage of plaque development. In addition, the third and most advanced stage is characterized by plaque rupture. In this stage, apoptosis and necrosis of macrophage-derived and SMC-derived foam cells lead to extracellular lipid accumulation and formation of a lipid necrotic core that expands and distends the plaque. In conjunction with proteolytic metalloproteinases secreted by the macrophages, this results in disruption of the fibrous plaque and ultimately in plaque rupture [70]. Plaque calcification usually occurs in this advanced stage and may develop from a passive process of dystrophic calcification or an active process of calcium formation by SMC-derived osteoblast-like cells [71]. Plaque rupture

exposes the collagen and lipid core to the lumen of the blood vessel, inducing platelet aggregation, coagulation, and thrombus formation, which could occlude the vessel at the site of the plaque or may embolize, causing downstream occlusions and infarction.

Based on the coronary and carotid literature, a vulnerable or unstable plaque is defined as a plaque that contains a large lipid necrotic core, intraplaque hemorrhage, and marked inflammation with a thin/ruptured fibrous cap separating the plaque contents from the lumen. In addition, these vulnerable plaques are usually associated with positive arterial remodeling. In contrast, stable plaques possess a higher fibrous component, a smaller lipid necrotic core, and fewer inflammatory cells, and the contents of a stable plaque are usually separated from the arterial lumen by a thick fibrous cap [72,73]. A histologic study of MCA plaques in symptomatic and asymptomatic patients showed similarities in plaque characteristics to the extracranial carotid arteries, with vulnerable symptomatic MCA plaques showing higher degrees of stenosis, greater lipid content (>40% of plaque), intraplaque hemorrhage, neovascularization, and increased thrombus compared with asymptomatic plaques. Degree of stenosis, lipid content, and neovascularization were independent predictors for MCA infarction [74]. High-resolution VWI is the only imaging technique with the potential to characterize plaque components and allow clinicians to differentiate vulnerable, unstable versus stable plaques. Table 2 outlines the signal intensities of different plaque components as described in the carotid VWI literature [74]. Preliminary studies have reported similar imaging characteristics among ICAD plaques.

INTRACRANIAL ATHEROSCLEROTIC DISEASE STROKE MECHANISMS

Ischemic strokes have been grouped into 5 clinical types according to the TOAST (Trial of Org 10172 in Acute Stroke Treatment) classification: (1) large artery atherosclerosis, (2) cardioembolic, (3) small-vessel occlusion (lacunar infarcts), (4)stroke with other rare cause (eg, dissection and arteritis), and (5) stroke of undetermined cause or cryptogenic stroke [78]. Most nonlacunar strokes are thromboembolic, and common sources of emboli include the heart, venous thrombosis with paradoxic embolism, or any non-occlusive atherosclerotic plaque from the aorta to the cervical and cerebral arteries [79]. Intracranial atherosclerosis can result in 3 different types of ischemic stroke via unique mechanisms that are not mutually exclusive:

1. Thromboembolic (artery to artery) stroke secondary to plaque rupture and fragmentation producing scattered or large arterial territory infarct
2. Lacunar (perforator) infarcts secondary to plaque overgrowth/rupture and local occlusion of perforator artery ostia
3. Hypoperfusion (watershed or border-zone) infarcts resulting from arterial lumen stenosis and flow limitation with failure of the collaterals to maintain cerebral blood flow to the affected territory [80]

TABLE 2
Signal intensities of different plaque components in multicontrast–weighted images from the carotid literature

	3D TOF MRA	T1WI	T2WI	PD weighted	Postcontrast
Fibrous Cap	Iso/hypo	Iso	hyper	Iso/hyper	Enhance
Intraplaque Hemorrhage (Acute→ Subacute → Chronic)	Hyper → hyper → hypo	Hyper → hyper →hypo	Iso/hypo → hyper →hypo	Iso/hypo → hyper →hypo	–
Lipid Necrotic Core	Iso	Iso/hyper	Hypo	Hyper	–
Calcification	Hypo	Hypo	Hypo	Hypo	–
Neovascularization	—	—	—	—	Enhance
Inflammation	—	—	—	—	Enhance

Abbreviations: 3D, three-dimensional; hyper, hyperintense; hypo, hypointense; iso, isointense; PD, proton density; TOF, time of flight; T1WI, T1-weighted imaging; T2WI, T2-weighted imaging.

Data from Refs [75–77].

Arterioembolic infarcts caused by plaque rupture usually occur in vulnerable plaques that contain larger lipid-rich necrotic cores and intraplaque hemorrhage with thin fibrous caps. Patients with these vulnerable plaques can benefit from plaque-stabilizing medical therapy, including aspirin and statins [81]. In contrast, patients with stable plaques (containing smaller lipid necrotic cores with more fibrous tissue and thicker fibrous cap) but causing high-grade, flow-limiting stenoses and tissue hypoperfusion may benefit from endovascular revascularization procedures. However, endovascular angioplasty/stenting of vulnerable plaques probably increases the risk of intraprocedural complications caused by plaque/thrombus disruption with embolic or perforator ischemic complications. The differentiation between stable and unstable/vulnerable plaques and the mechanism of ischemic stroke is critical for the proper clinical triage and recurrent stroke prevention in these patients.

MAGNETIC RESONANCE VESSEL WALL IMAGING PROTOCOLS

Several factors must be considered in developing an optimized MR VWI protocol:

1. Blood and CSF nulling techniques to achieve the best contrast/noise ratio (CNR)
2. Minimum required spatial resolution for accurate diagnosis
3. Two-dimensional (2D) versus three-dimensional (3D) imaging
4. T1- weighted imaging (T1WI)/T2-weighted imaging sequences
5. MR field strength required to achieve diagnostic CNR and SNR within institutional time constraints [82]

Blood and Cerebrospinal Fluid Suppression

For optimal image contrast, blood and CSF suppression techniques must be properly implemented for adequate depiction of the inner and outer walls of blood vessels [82]. Black-blood nulling as a result of intravoxel dephasing is an innate property of 3D turbo spin echo (TSE) sequences with variable flip angle refocusing pulses and is the most commonly used blood suppression technique [57,83,84]. Other techniques include the use of preparation pulse protocols, including double inversion recovery (DIR) [85], delay alternating with nutation for tailored excitation (DANTE) [86], and flow-sensitive dephasing [87]. Although the use of preparation techniques such as DANTE has been shown to improve image contrast secondary to better blood suppression [88,89], their application increases imaging time. A tradeoff between acquisition time and the optimum degree of blood suppression must be optimized, with an ideal sequence achieving the best CNR with the shortest scanning time possible [82].

CSF suppression is most commonly achieved with techniques that suppress signal based on CSF flow [88,89]. However, these standard techniques are suboptimal in areas of low CSF flow and volume, such as the skull base, and optimal CSF suppression remains an active area of research and development. A new suppression technique using an anti–driven equilibrium pulse that depends on the innate T1 and T2 relaxation properties of CSF rather than flow is promising to improve CSF suppression with 3-T MRI [90,91]. Inversion recovery pulse sequences can provide excellent CSF suppression, but their application is time consuming, and they can have a detrimental effect on SNR, which has traditionally limited these protocols to 7-T MRI machines [42]. However, using parallel imaging and the phase undersampling GRAPPA (GeneRalized Autocalibrating Partial Parallel Acquisition) technique, an inversion recovery 3D-SPACE (Sampling Perfection with Application optimized Contrasts using different flip angle Evolution) (IR-SPACE) sequence has been developed that allows for complete brain coverage with excellent CSF suppression and vessel wall–CSF contrast in a reasonable scan time on a 3-T magnet [90], and remains an active area of future research.

Spatial Resolution

A consensus has not yet been reached regarding the optimal spatial resolution for plaque detection and for the accurate assessment of vessel wall disease. However, it is generally accepted that characterization of objects on MRI requires at least 2 voxels within the object of interest to minimize the effects of partial volume averaging [92]. In addition, in blood vessels, a minimum of 2 voxels is required within the vessel lumen to isolate a focal vessel wall lesion from the opposing wall [93]. A histopathologic study has shown the internal carotid artery (ICA) diameter to range between 3.0 and 4.8 mm, and the MCA diameter to range between 2.3 and 3.5 mm. The same study showed a wall thickness between 0.3 and 0.7 mm for the ICA and between 0.3 and 0.5 mm for the MCA [94]. An alternative histologic study has reported MCA wall thicknesses to range between 0.5 and 0.7 mm [95]. In an ex vivo vessel wall imaging study using an ultrahigh-resolution VWI protocol with 0.11-mm and 0.13-mm isotropic voxels on 7-T

MRI to detect vessel wall thickness, the mean vessel wall thickness in the circle of Willis was 0.45 mm (0.31–0.52 mm), showing excellent agreement with histologic assessments. Thus, to obtain 2 voxels within the wall of the MCA would require MRI with isotropic voxels as small as 0.15 mm for accurate VWI assessment [82]. Executing VWI protocols with such an ultrahigh resolution requires the use of 7-T MRI and significantly prolonged acquisition times, which at this time have been limited to research purposes. In clinical practice, most experts agree that a VWI protocol with isotropic 0.4-mm to 0.7-mm voxels is adequate for diagnosis [96].

Two-Dimensional Versus Three-Dimensional Protocols

Because of the complex anatomy and tortuosity of intracranial vessels, most experts prefer 3D acquisition sequences to 2D protocols. 3D sequences offer the advantage of imaging the entire intracranial vasculature within a reasonable scan time, better through-plane resolution, and isotropic voxel acquisition that allows multiplanar reformatting [52,57,82,83,96,97]. However, higher in-plane spatial resolution can be achieved using 2D imaging, and, although 2D imaging lacks through-plane resolution, this can be mitigated by acquiring 2D sequences in multiple orthogonal planes [98]. In order to acquire multiple orthogonal 2D sequences within a reasonable scan time, it is necessary to limit the field of view and to determine the correct oblique positioning to target a specific lesion. This process requires increased time and expertise during image acquisition and is suboptimal for initial screening studies. Nonetheless, 2D imaging may have a role for interrogating specific vessel wall lesions, or for follow-up of patients with known vessel wall disease.

Field Strength

Field strength is another important factor in VWI. Most centers use 3-T MRI because it offers adequate spatial resolution, CNR, and SNR in reasonable scan times. Expert guidelines indicate that 1.5-T MRI provides suboptimal SNR and CNR to achieve diagnostically adequate VWI [82,96]. 7-T MRI has recently been used in VWI and offers superior image quality because of better SNR, CNR, and CSF suppression techniques [42,99,100]. However, because of its rare availability in the clinical setting, 7-T VWI is currently used only for research purposes and 3-T MRI remains the standard field strength.

Image Weighting

Extracranial carotid VWI protocols are well established, and the use of 3D time-of-flight (TOF) MRA combined with multicontrast black-blood pulse sequences (T1, T2, PD, and T1 postcontrast) and fat suppression is recommended for delineation of various plaque characteristics [73]. Mimicking the extracranial protocols, intracranial VWI typically uses similar multicontrast sequences to provide an adequate characterization of the underlying vascular disorder [101]. However, the acquisition of multiple sequences of various T1 and T2 weightings requires longer scan times, which not only increases the cost of the imaging study to the radiology department but also increases patient discomfort and resultant motion artifacts [102]. In carotid VWI, a single 5-minute Multi-contrast Atherosclerosis Characterization (MATCH) scan protocol has been described in which interleaved T1-weighted, gray blood, and T2-weighted images are acquired in a single repetition time to limit scan times [103]. The possibility of implementing similar scan techniques in the intracranial circulation has yet to be studied. At present, in order to minimize scan times, most centers use streamlined VWI protocols with 3D TOF MRA and a T1-weighted black-blood sequence pre- and post-contrast, which was shown to be the single most effective sequence in distinguishing various intraplaque components [104]. Unlike extracranial VWI, the use of fat suppression is not essential in intracranial VWI [96].

Contrast Injection

The use of gadolinium-based contrast agents in MR VWI is critical, but the optimal scanning time after contrast injection has not yet been determined. Very early acquisitions after contrast injection can be limited by weak plaque enhancement, whereas delayed acquisitions may result in indiscriminate enhancement of all unstable and stable atherosclerotic plaques. Although preliminary results have suggested a peak CNR at 20 minutes [105], most centers use a VWI protocol in which post-contrast sequences are initiated 5 to 10 minutes after contrast administration [43,83,84,97].

Pulse Gating

Several research studies have used pulse sequence cardiac gating in VWI to optimize blood suppression by gating the acquisition to the time of maximal flow within the vessel, but such protocols have not yet been integrated into routine clinical practice [96,106].

Among the MR VWI sequences that have been developed by various vendors, 3D variable refocusing

TABLE 3
3-T magnetic resonance vessel wall imaging protocol

Imaging Parameter	3D TOF MRA	3D T1 TSE (SPACE) Pre- and Post-contrast	3D T2 TSE (SPACE)
FOV (mm^3) or (cm)	200	165	230
Matrix	296 × 384	320 × 320	320 × 320
Slice thickness (mm)	0.5	0.6	0.7
In-plane resolution (mm)	0.26 × 0.26	0.5 × 0.5	0.7 × 0.7
Acquisition orientation	Axial oblique	Axial	Sagittal
Acquisition spatial resolution (mm^3)	0.5 × 0.5 × 1	0.5 × 0.5 × 0.8	0.7 × 0.7 × 0.7
Reconstruction spatial resolution (mm^3)	0.26 × 0.26 × 0.5	0.5 × 0.5 × 0.6	0.7 × 0.7 × 0.7
TR/TE (ms)	22/3.4	800/23	3200/371
Flip angle (°)	17 (15–19)	Variable	Variable
Echo spacing (ms)	—	167	3.8
TSE factor	—	30	282
Bandwidth	186	372	679
Number of averages	1	1.6	1
Acquisition time	7 min 57 s	7 min 24 s	7 min 17 s

Abbreviations: FOV, field of view; TE, echo time; TR, repetition time.

flip angle sequences are the most extensively used because of their superior image quality and brain coverage with reasonable scan times (CUBE, GE Healthcare, Milwaukee, WI; SPACE [Sampling Perfection with Application optimized Contrasts using different flip angle Evolution], Siemens Healthcare, Erlangen, Germany; VISTA [Volume ISotropic Turbo spin echo Acquisition], Philips Healthcare, Best, the Netherlands) [106]. At our institution, we use noncontrast T2-SPACE, and precontrast and postcontrast T1 SPACE sequences, with imaging parameters detailed in Table 3.

MAGNETIC RESONANCE VESSEL WALL IMAGING: NORMAL INTRACRANIAL VASCULATURE

Normal vessel walls are visualized as thin structures isointense to surrounding white matter with black blood centrally within the vessel lumen. With aging and brain atrophy, increasing CSF surrounds the vessel wall improving visualization because of a higher CNR with CSF suppression techniques. Identifying vessel wall disorder depends on the presence of 1 or more of the following abnormalities:

1. Focal (eccentric) or diffuse (concentric) vessel wall thickening [54]
2. Signal hyperintensity on pre-contrast images [107]
3. Focal (eccentric) or diffuse (concentric) contrast enhancement [97]

Some intracranial arteries show normal periarterial enhancement, which must not be confused for pathology. In a study of a pediatric population, normal periarterial enhancement was noted in the petrous and cavernous segments of the ICA and the M1 segment of the MCA (Fig. 1). Such enhancement is typically bilateral and may be attributed to the presence of dural meninges bordering the arteries at these locations or to periarterial veins [108]. An alternative explanation for normal arterial enhancement in the petrous ICA and the vertebral arteries is the presence of vasa vasorum at the transition point between the extracranial and intracranial segments of these vessels [56].

In addition to normal periarterial enhancement, MR artifacts may mimic disorder in a normal vessel wall. In laminar flow, the slowest moving blood is located adjacent to the vessel wall. MR VWI techniques that depend solely on flow for nulling the blood signal may result in suboptimal suppression at the periphery of the vessel, creating the artifactual appearance of wall

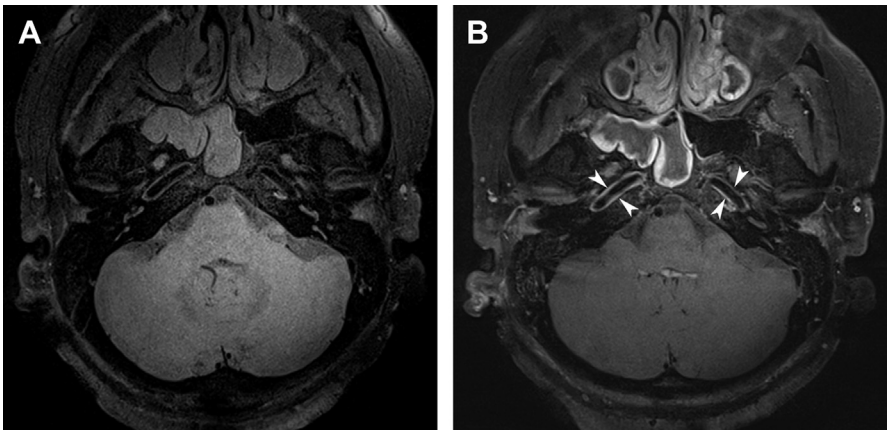

FIG. 1 High-resolution MR VWI with black-blood MRI (BBMRI) axial (**A**) precontrast and (**B**) postcontrast images showing patent bilateral internal carotid arteries and basilar arteries with normal intraluminal hypointensity (black blood) and normal bilateral vessel wall enhancement in the horizontal petrous segment of the internal carotid arteries (*arrowheads*) on postcontrast images.

thickening or enhancement [82]. Suboptimal suppression of slow flow in the intracranial veins that are immediately adjacent to cerebral arteries can also mimic focal lesions.

MAGNETIC RESONANCE VESSEL WALL IMAGING: INTRACRANIAL ATHEROSCLEROTIC DISEASE

As previously described, atherosclerotic plaques have a complex composition with variable degrees of lipid necrotic core, fibrous tissue, intraplaque hemorrhage, and inflammatory cells. Plaque activity and stability are determined by the variations in the amounts of these components within the plaque. The use of MR VWI for characterizing vulnerable cervical carotid artery plaques has been well established by research that validated the in vivo MRI studies with histologic analysis of ex vivo carotid artery specimens obtained during carotid endarterectomy [109]. Although no intervention similar to cervical carotid endarterectomy currently exists for the intracranial circulation, several studies with histologic validation have shown the accuracy and reliability of in vivo VWI in detecting intracranial atherosclerosis [110–114].

In an early study of symptomatic MCA stenosis using 1.5-T high-resolution MRI (HR-MRI), T1 and T2 black-blood axial images detected intracranial plaques as eccentric (crescentlike) wall thickness with intense postcontrast enhancement at the site of maximum stenosis. In comparison, non-stenotic MCA segments showed neither wall thickness nor enhancement [115]. Those findings were later confirmed in a study by Swartz and colleagues [54] in which multicontrast HR VWI was performed on a 3-T MRI with the aim of differentiating intracranial vasculopathies presenting with intracranial stenosis. Swartz and colleagues [54] reported that more than 90% of patients with ICAD showed eccentric vessel wall thickening and that 75% of plaques showed enhancement only in vessels implicated in the ischemic injury.

Xu et al [116] studied the prevalence of intraplaque hemorrhage in ICAD and its clinical significance using HR-MRI. Intraplaque hemorrhage was defined as hyperintense signal on noncontrast T1WI and was observed in 10.1% of patients with MCA stenosis. Furthermore, lesions with intraplaque hemorrhage were shown to be highly associated with ipsilateral strokes. This finding was further supported in another study where postmortem histopathologic findings identified higher rates of intraplaque hemorrhage (30% vs 15%) in culprit versus non-culprit atherosclerotic plaques [74].

Higher lipid content (>40% by area) within intracranial MCA atherosclerotic plaques has been shown to represent an independent risk factor for MCA territory infarcts [74]. In an ex vivo multicontrast 3-T HR-MRI study of intracranial vessels, T2 and T2* pulse sequences were able to differentiate lipid core (hypointense on T2 and T2*) from the fibrous cap (hyperintense on T2 and T2*) with good interobserver agreement and correlation with histology [117]. Similar findings were shown in several in vitro studies assessing ICAD plaques using ultrahigh-resolution 7-T MR VWI protocols with histopathologic validation. These

studies showed that fibrous caps show a T2 hyperintense juxtaluminal band, whereas lipid necrotic cores show T2 hypointense signal [110,114]. Mossa-Basha and colleagues [101] studied 29 patients with clinically defined intracranial vasculopathies (atherosclerosis, vasculitis, and reversible cerebral vasoconstriction syndrome [RCVS]) using multicontrast 3-T HR-MRI and found that only patients with known atherosclerosis showed intralesional T2 hyperintensity. The sensitivity of VWI to differentiate intracranial atherosclerosis from other vasculopathies was a promising 96.3% with the combined use of T1WI and T2-weighted imaging [101].

In the coronary and extracranial carotid literature, intraplaque calcification has been found to be associated with more complex and unstable plaques [118]. A paucity of data exists for calcification in the intracranial arteries, but one study showed calcification rates as high as 28% in the MCAs, with a higher prevalence of calcification in symptomatic lesions compared with asymptomatic MCA stenoses (35% vs 23%) [74]. There are even fewer data regarding the prevalence and appearance of intracranial calcification on MR VWI and its correlation with symptomatic and asymptomatic plaques.

Intraplaque contrast enhancement has been postulated to correlate with the degree of inflammation and neovascularization within atherosclerotic plaques and has been linked to a higher probability of ischemic events (Fig. 2) [119]. Because the pituitary stalk

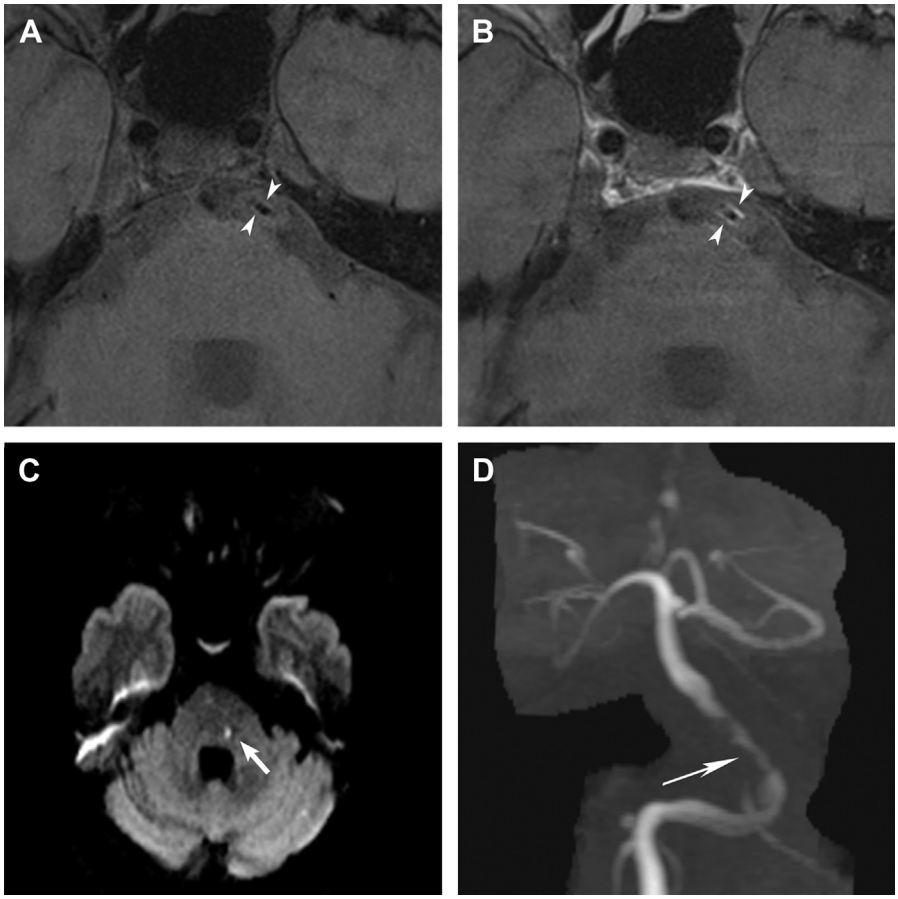

FIG. 2 A 67-year-old patient presents with expressive aphasia and right hemiparesis. (**A**) BBMRI axial precontrast image shows marked segmental narrowing of the basilar artery with irregular vessel wall enhancement (*arrowheads*) on (**B**) postcontrast BBMRI image. (**C**) MR DWI image shows a left pontine focus of restricted diffusion corresponding with a perforator type infarct (*thick arrow*). (**D**) 3D TOF MRA image confirms the marked narrowing and irregularity in the lower half of the basilar artery (*thin arrow*), suggestive of an inflammatory and unstable ICAD plaque.

normally enhances intensely with contrast [120], many studies have used it as an internal reference to determine the degree of plaque/lesion enhancement. In one influential study investigating the relationship between plaque enhancement and ischemic events, intracranial plaque enhancement was classified into 3 grades (grade 0, no enhancement; grade1, enhancement less than pituitary infundibulum; and grade 2, enhancement equal to or greater than the pituitary infundibulum). Grade 2 enhancement was associated with culprit plaques, whereas grade 0 was only observed in non-culprit plaques, suggesting a strong correlation between the degree of enhancement and plaque stability [97]. Another study compared plaque enhancement in acute, subacute, and chronic phases of ischemic injury, and showed that the presence and strength of plaque enhancement decreased over time, showing a correlation between acute ischemic stroke and plaque enhancement [121]. This finding suggests that enhancement reflects an ongoing process of inflammation and neovascularization in acute symptomatic plaques and may indicate a role for MR VWI in assessing the treatment response in such patients.

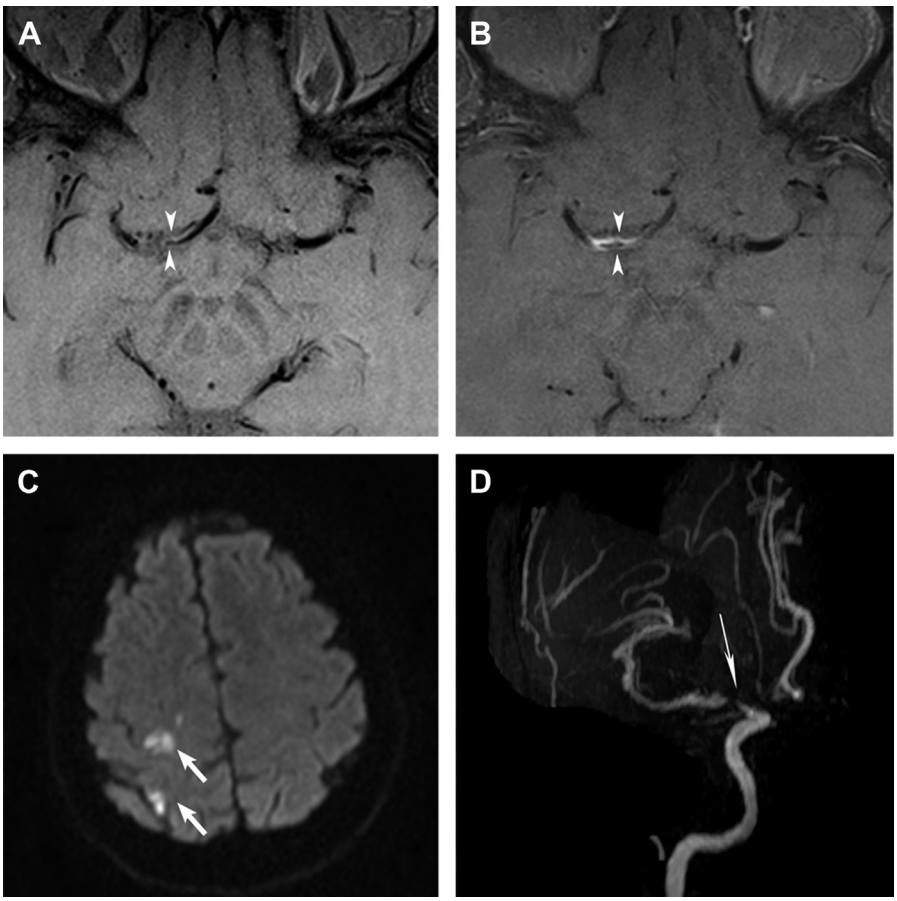

FIG. 3 A 57-year-old patient with history of right parietal infarction. (**A**) BBMRI axial precontrast image shows patent, but markedly narrowed, right ICA terminus with extension of ICAD-related stenosis into the proximal A1 and M1 segments. In addition, high-grade vessel wall hyperintensity (*arrowheads*) corresponding with high-grade enhancement (*arrowheads*) on (**B**) postcontrast BBMRI images is suggestive of an active plaque with intraplaque hemorrhage. (**C**) MR DWI image shows new right parietal foci of restricted diffusion (*thick arrow*) characteristic of a thromboembolic pattern of infarction. (**D**) 3D TOF MRA image shows a false-positive finding of a right ICA terminus (*thin arrow*) occlusion caused by low-flow artifact and poor intravascular flow enhancement secondary to a severe ICAD stenosis that was accurately diagnosed on a high-resolution MR VWI.

TABLE 4
Imaging criteria of vessel wall disorder on luminal angiography and magnetic resonance vessel wall imaging

	Luminal Angiography	Disease Pattern	T1WI	T2WI	Contrast Enhancement	Affected Vessels	Other Findings	Outer wall Remodeling	Follow-up	Overlapping Findings
Dissection [130–136] (Fig. 4)	Tapered irregular stenosis often presents with focal aneurysmal dilatation, intimal flap, and double lumen could be seen	Eccentric (rarely concentric)	Hyperintense (if intramural hematoma)	Variable	± (more commonly present)	Any artery (most commonly affected: distal ICA, vertebral)	Intimal flap, double lumen, intramural hematoma, aneurysmal dilatation	Positive followed by restoration	Complete recanalization rates from 18% (2 mo) up to 62% (6 mo)	ICAD
ICAD [50,97,107, 112,116,119, 121,137,138]	Stenotic segments with irregular lumen and ulcerations, or normal looking vessels (outward remodeling)	Eccentric (rarely concentric)	Hyperintense (if intraplaque hemorrhage)	Juxtaluminal T2 hyperintensity	Depend on stage (+++ → −)	Widespread	Plaque characterization depends on plaque components (see Table 2)	Positive and negative remodeling	Regression in 58% of patients, but normalization in <35% with aggressive medical therapy	Vasculitis/ dissection
Vasculitis [101, 139–141]	Focal or multifocal segmental stenosis of the affected vessels with possible occlusion	Concentric (rarely eccentric)	–	Isointense	++ (resolves with treatment)	Widespread with long segment affection of medium and small sized vessels	Usually, diagnosis of exclusion, site of enhancement can guide biopsy	—	One-third resolve with treatment over 6–7 mo	Atherosclerosis/ RCVS
RCVS [101, 139,141]	Alternating areas of smooth, tapered narrowing and dilatation in the affected artery (string of beads on angiogram)	Concentric (rarely eccentric)	–	isointense	± (more commonly absent)	Widespread affection of medium to small sized vessels	Diagnosis of exclusion	Negative	90% Spontaneously resolve in 8–12 wk	Vasculitis

Moyamoya [51, 142–144]	steno-occlusive disease of the affected vessels with multiple collaterals ("puff of smoke")	Concentric	–	–	±	Terminal ICA, proximal MCA	Can be unilateral but usually bilateral	Negative	Progressive	Vasculitis
IA [55,93, 145–148]	Saccular or fusiform arterial dilatation	–	Hyperintense (in areas of increased wall thickness and intramural hematoma)	–	+ (at sites of rupture)	Saccular aneurysms occur at bifurcation points (Acom>supraclinoid ICA>MCA >Posterior circulation)	IA thrombus could be identified Identify ruptured aneurysm causing SAH in patients with multiple aneurysms identify blood blister aneurysms	Positive remodeling	Stationary or progressive increase in size if left untreated	–
Post-thrombectomy	Normal-looking vessel (might show partial filling defect with residual thrombus or irregularities if underlying ICAD or dissection)	Concentric (rarely eccentric)	–	–	+ (concentric focal enhancement at the treated vessel)	Terminal ICA, proximal MCA	Enhancement is associated with the type of device, number of thrombectomy attempts, and could predict postprocedure hemorrhagic transformation	–	–	Vasculitis

Abbreviations: Acom, Anterior communicating artery; ICAD, Intracranial atherosclerotic disease; IA, intracranial aneurysms; RCVS, reversible cerebral vasoconstriction syndrome; SAH, subarachnoid hemorrhage.

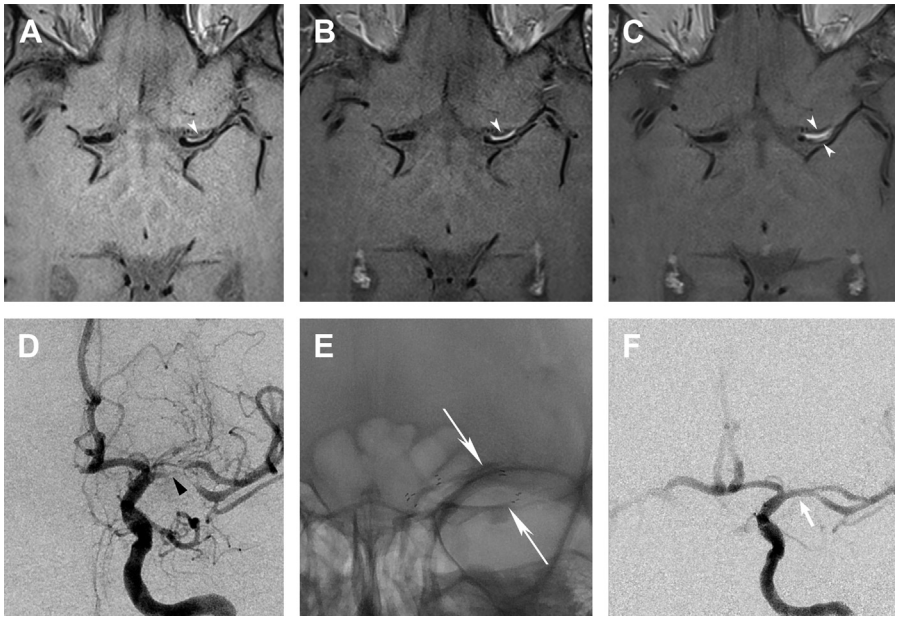

FIG. 4 A 53-year-old patient with history of left frontotemporal headaches followed by word-finding difficulties. (**A**) BBMRI axial precontrast and (**B**) postcontrast images show long-segment, eccentric hyperintensity, and avid contrast enhancement (*white arrowheads*) along the anterior wall of the left MCA concerning for an intracranial dissection versus less likely intracranial atherosclerosis. (**C**) BBMRI postcontrast image 1 month after angioplasty shows recurrent long-segment spiral stenosis with long spiral (*white arrowheads*) with persisting strong enhancement. (**D**) DSA anteroposterior (AP) image 1 month after angioplasty confirms a nonhealing intracranial dissection flap (*black arrowhead*) causing restenosis of the left MCA M1 segment extending to proximal M2 segments. (**E**) Native fluoroscopy image shows interval deployment of 2 intracranial stents (*thin arrows*) from the left M1 into each of the superior and inferior M2 division segments. (**F**) Posttreatment DSA AP image confirms stent reconstruction of the vessel wall with restoration of the normal MCA caliber (*thick arrow*) and no residual intracranial dissection-related stenosis, intimal flap, or flow limitation.

Plaque enhancement also correlated with the pattern of infarction. An initial study showed that enhancing plaques are more commonly associated with scattered arterioembolic infarcts (Fig. 3), whereas nonenhancing plaques are more commonly associated with small vessel lacunar infarcts [122]. Wu and colleagues [123] confirmed these findings and also reported intraplaque enhancement to be the strongest independent predictor of artery-to-artery embolic infarction. Furthermore, they showed that a more peripheral juxtaluminal plaque enhancement is highly correlated with an artery-to-artery embolism mechanism compared to a deep in-plaque pattern of enhancement (66.7% vs 33.3%) [123]. These findings further support plaque enhancement as a sign of vulnerability and suggest a possible benefit from plaque-stabilizing treatments such as anti-inflammatory drugs and statins.

Atherosclerosis is a chronic inflammatory process in which T lymphocytes and monocytes play a major role in plaque formation, progression, and destabilization. Ferumoxytol is a superparamagnetic iron oxide nanopeptide that generates a hypointense signal on T2* gradient-recalled echo sequences and a hyperintense signal on T1WI. It is cleared from the blood by macrophages, and it can be used to detect the abundance and phagocytic activity of macrophages within atherosclerotic plaques [124]. A pilot study evaluated early (within 24 hours) and late (within 72 hours) uptake of ferumoxytol in cerebral aneurysm walls and found higher rupture rates for cerebral aneurysms displaying early ferumoxytol uptake [125]. Similarly, ferumoxytol-enhanced HR-MRI may be able to detect vulnerable plaques with active inflammation and to assess their response to anti-inflamatory medications

and treatment. This topic represents a fertile area for future research.

MAGNETIC RESONANCE VESSEL WALL IMAGING IN DIFFERENTIATING INTRACRANIAL STENOSES, OCCLUSIONS, AND VASCULOPATHIES

MR VWI can accurately detect the degree of arterial stenosis and occlusion with high sensitivity and specificity, and good interobserver and intraobserver agreement [126–128]. Liu et al [126] showed that high-resolution VWI was able to detect MCA stenosis greater than 50% with higher sensitivity than CTA using DSA as the gold standard. Another group studied the diagnostic accuracy of black-blood luminal angiography (BBLA), which is a minimal intensity reconstruction of vessel wall source images, in detecting the degree and length of stenosis compared with source images and TOF MRA and showed that VWI (BBLA and source images) had higher sensitivity and specificity in detecting severe stenosis and occlusion compared with TOF MRA. BBLA also showed greater accuracy in the assessment of the length of stenosis compared with CTA [127]. Baik et al [129] characterized the MR VWI imaging findings of arterial occlusions as being distinct from intracranial stenoses in patients with acute ischemic stroke, specifically concentric, round, and longer segments of strong T1-weighted enhancement.

Apart from the ability to characterize ICAD plaques as detailed earlier, MR VWI can also differentiate atherosclerotic plaques from alternative intracranial vasculopathies that may require different targeted treatments. Table 4 provides a summary of the imaging findings for different intracranial vascular diseases on luminal angiography and MR VWI.

MAGNETIC RESONANCE VESSEL WALL IMAGING LIMITATIONS AND FUTURE CONSIDERATIONS

Intracranial MR VWI is a novel state-of-the-art imaging technique, and its clinical utility is steadily increasing. It promises to aid in the identification and characterization of intracranial vasculopathies that cannot be assessed by traditional imaging techniques, but intracranial VWI also faces significant limitations. For imaging of the extracranial carotid artery, validation of in vivo VWI findings can be easily performed against the readily available histologic specimens obtained from carotid endarterectomies. However, no similar procedure, and thus correlation, exists for the intracranial vasculature, making in vivo validation of intracranial VWI findings much more challenging. Several studies have attempted to validate ex vivo findings of HR VWI [110,114], but these studies suffer from a paucity of data and significant technical limitations, including the inability to test imaging characteristics such as postgadolinium contrast enhancement in postmortem studies and the unknown effect of histologic tissue preparation techniques on the MR signal of different plaque components.

Another important challenge for intracranial VWI arises from the small size and pronounced tortuosity of the small intracranial vessels. This challenging anatomy requires a high isotropic spatial resolution as well as excellent blood and CSF suppression for adequate CNR. These requirements substantially increase scan times, which strains hospital resources and leads to patient discomfort and motion artifacts. As previously described, several technical imaging advancements and innovative methods have enabled the reduction of scan times without a detrimental effect on image quality. These promising imaging protocols include improved CSF suppression techniques such as DANTE and anti–driven equilibrium techniques [86,88–91], compressed sensing k-space sampling, and advanced parallel imaging techniques [57,149,150].

SUMMARY

High-resolution MR VWI is a promising tool for the diagnosis and management of intracranial atherosclerotic disease 3-T MR VWI is able to evaluate in vivo atherosclerotic plaques and provide insight for differentiation of vulnerable from stable plaques based on their signal intensity and enhancement characteristics. It can provide useful diagnostic and prognostic information regarding a patient's future stroke risk, and it can assist in determining targeted treatment options for optimal patient care.

ACKNOWLEDGMENTS

This work was supported by the following grants: American Heart Association 13GRNT17340018, 14GRNT20380798 (principal investigators: S.A. Ansari and T.J. Carroll); National Institutes of Health (NIH)/NHLBI 1R21HL130969 (principal investigator: S.A. Ansari); and NIH/NINDS 1R01NS093908 (principal investigator: T.J. Carroll).

REFERENCES

[1] Gorelick Philip B, Wong KS, Bae HJ, et al. Large artery intracranial occlusive disease: a large worldwide burden

but a relatively neglected frontier. Stroke 2008;39(8):2396–9.
[2] Benjamin EJ, Blaha MJ, Chiuve SE, et al. Heart disease and stroke statistics-2017 update: a report from the American Heart Association. Circulation 2017;135(10):e146–603.
[3] Kasner Scott E, Chimowitz MI, Lynn MJ, et al. Predictors of ischemic stroke in the territory of a symptomatic intracranial arterial stenosis. Circulation 2006;113(4):555–63.
[4] Sacco RL, Kargman DE, Gu Q, et al. Race-ethnicity and determinants of intracranial atherosclerotic cerebral infarction. The Northern Manhattan Stroke Study. Stroke 1995;26(1):14–20.
[5] Caplan LR, Gorelick PB, Hier DB. Race, sex and occlusive cerebrovascular disease: a review. Stroke 1986;17(4):648–55.
[6] Chimowitz MI, Kokkinos J, Strong J, et al. The Warfarin-Aspirin symptomatic intracranial disease study. Neurology 1995;45(8):1488–93.
[7] Suri MF, Johnston SC. Epidemiology of intracranial stenosis. J Neuroimaging 2009;19(Suppl 1):11s–6s.
[8] Bos D, van der Rijk MJ, Geeraedts TE, et al. Intracranial carotid artery atherosclerosis: prevalence and risk factors in the general population. Stroke 2012;43(7):1878–84.
[9] White H, Boden-Albala B, Wang C, et al. Ischemic stroke subtype incidence among whites, blacks, and Hispanics: the Northern Manhattan Study. Circulation 2005;111(10):1327–31.
[10] Wong KS, Huang YN, Gao S, et al. Intracranial stenosis in Chinese patients with acute stroke. Neurology 1998;50(3):812–3.
[11] Wong Ka S, Li H, Chan YL, et al. Use of transcranial doppler ultrasound to predict outcome in patients with intracranial large-artery occlusive disease. Stroke 2000;31(11):2641–7.
[12] Huang YN, Gao S, Li SW, et al. Vascular lesions in Chinese patients with transient ischemic attacks. Neurology 1997;48(2):524–5.
[13] De Silva DA, Woon FP, Lee MP, et al. South Asian patients with ischemic stroke: intracranial large arteries are the predominant site of disease. Stroke 2007;38(9):2592–4.
[14] Kaul S, Sunitha P, Suvarna A, et al. Subtypes of ischemic stroke in a metropolitan city of South India (one year data from a hospital based stroke registry). Neurol India 2002;50(1):S8–15.
[15] Wong KS, Ng PW, Tang A, et al. Prevalence of asymptomatic intracranial atherosclerosis in high-risk patients. Neurology 2007;68(23):2035–8.
[16] Uehara T, Tabuchi M, Mori E. Frequency and clinical correlates of occlusive lesions of cerebral arteries in Japanese patients without stroke. Evaluation by MR angiography. Cerebrovasc Dis 1998;8(5):267–72.
[17] Leung SY, Ng TH, Yuen ST, et al. Pattern of cerebral atherosclerosis in Hong Kong Chinese. Severity in intracranial and extracranial vessels. Stroke 1993;24(6):779–86.
[18] Qureshi AI, Caplan LR. Intracranial atherosclerosis. Lancet 2014;383(9921):984–98.
[19] Huang HW, Guo MH, Lin RJ, et al. Prevalence and risk factors of middle cerebral artery stenosis in asymptomatic residents in Rongqi County, Guangdong. Cerebrovasc Dis 2007;24(1):111–5.
[20] Bae HJ, Lee J, Park JM, et al. Risk factors of intracranial cerebral atherosclerosis among asymptomatics. Cerebrovasc Dis 2007;24(4):355–60.
[21] Tsivgoulis G, Vadikolias K, Heliopoulos I, et al. Prevalence of symptomatic intracranial atherosclerosis in Caucasians: a prospective, multicenter, transcranial Doppler study. J Neuroimaging 2014;24(1):11–7.
[22] Ovbiagele B, Saver JL, Lynn MJ, et al. Impact of metabolic syndrome on prognosis of symptomatic intracranial atherostenosis. Neurology 2006;66(9):1344–9.
[23] Park JH, Kwon HM, Roh JK. Metabolic syndrome is more associated with intracranial atherosclerosis than extracranial atherosclerosis. Eur J Neurol 2007;14(4):379–86.
[24] Bang OY, Lee MA, Lee JH, et al. Association of the metabolic syndrome with intracranial atherosclerotic stroke. Neurology 2005;65(2):296–8.
[25] Hallevi H, Chernyshev OY, El Khoury R, et al. Intracranial atherosclerosis is associated with progression of neurological deficit in subcortical stroke. Cerebrovasc Dis 2012;33(1):64–8.
[26] Kang DW, Kwon SU, Yoo SH, et al. Early recurrent ischemic lesions on diffusion-weighted imaging in symptomatic intracranial atherosclerosis. Arch Neurol 2007;64(1):50–4.
[27] Qureshi AI, Ziai WC, Yahia AM, et al. Stroke-free survival and its determinants in patients with symptomatic vertebrobasilar stenosis: a multicenter study. Neurosurgery 2003;52(5):1033–9 [discussion: 1039–40].
[28] Kozak O, Tariq N, Suri MF, et al. High risk of recurrent ischemic events among patients with deferred intracranial angioplasty and stent placement for symptomatic intracranial atherosclerosis. Neurosurgery 2011;69(2):334–42 [discussion: 342–3].
[29] Wong KS, Li H. Long-term mortality and recurrent stroke risk among Chinese stroke patients with predominant intracranial atherosclerosis. Stroke 2003;34(10):2361–6.
[30] Brott TG, Hobson RW 2nd, Howard G, et al. Stenting versus endarterectomy for treatment of carotid-artery stenosis. N Engl J Med 2010;363(1):11–23.
[31] Ferguson Gary G, Eliasziw M, Barr HW, et al. The North American symptomatic carotid endarterectomy trial: surgical results in 1415 patients. Stroke 1999;30(9):1751–8.
[32] Chimowitz MI, Lynn MJ, Derdeyn CP, et al, SAMMPRIS Trial Investigators. Stenting versus aggressive medical therapy for intracranial arterial stenosis. N Engl J Med 2011;365(11):993–1003.

[33] Zaidat OO, Fitzsimmons BF, Woodward BK, et al, VISSIT Trial Investigators. Effect of a balloon-expandable intracranial stent vs medical therapy on risk of stroke in patients with symptomatic intracranial stenosis: the VISSIT randomized clinical trial. JAMA 2015;313(12):1240–8.
[34] Chimowitz MI, Lynn MJ, Howlett-Smith H, et al, Warfarin-Aspirin Symptomatic Intracranial Disease Trial Investigators. Comparison of warfarin and aspirin for symptomatic intracranial arterial stenosis. N Engl J Med 2005;352(13):1305–16.
[35] ESPRIT Study Group, Halkes PH, van Gijn J, Kappelle LJ, et al. Aspirin plus dipyridamole versus aspirin alone after cerebral ischaemia of arterial origin (ESPRIT): randomised controlled trial. Lancet 2006;367(9523):1665–73.
[36] ESPRIT Study Group, Halkes PH, van Gijn J, Kappelle LJ, et al. Medium intensity oral anticoagulants versus aspirin after cerebral ischaemia of arterial origin (ESPRIT): a randomised controlled trial. Lancet Neurol 2007;6(2):115–24.
[37] Wong KS, Chen C, Ng PW, et al, FISS-tris Study Investigators. Low-molecular-weight heparin compared with aspirin for the treatment of acute ischaemic stroke in Asian patients with large artery occlusive disease: a randomised study. Lancet Neurol 2007;6(5):407–13.
[38] Sacco RL, Diener HC, Yusuf S, et al, PRoFESS Study Group. Aspirin and extended-release dipyridamole versus clopidogrel for recurrent stroke. N Engl J Med 2008;359(12):1238–51.
[39] Kwon SU, Hong KS, Kang DW, et al. Efficacy and safety of combination antiplatelet therapies in patients with symptomatic intracranial atherosclerotic stenosis. Stroke 2011;42(10):2883–90.
[40] Nguyen-Huynh MN, Wintermark M, English J, et al. How accurate is CT angiography in evaluating intracranial atherosclerotic disease? Stroke 2008;39(4):1184–8.
[41] Bash S, Villablanca JP, Jahan R, et al. Intracranial vascular stenosis and occlusive disease: evaluation with CT angiography, MR angiography, and digital subtraction angiography. AJNR Am J Neuroradiol 2005;26(5):1012–21.
[42] van der Kolk AG, Zwanenburg JJ, Brundel M, et al. Intracranial vessel wall imaging at 7.0-T MRI. Stroke 2011;42(9):2478–84.
[43] Qiao Y, Anwar Z, Intrapiromkul J, et al. Patterns and implications of intracranial arterial remodeling in stroke patients. Stroke 2016;47(2):434–40.
[44] Glagov S, Weisenberg E, Zarins CK, et al. Compensatory enlargement of human atherosclerotic coronary arteries. N Engl J Med 1987;316(22):1371–5.
[45] Degnan AJ, Gallagher G, Teng Z, et al. MR angiography and imaging for the evaluation of middle cerebral artery atherosclerotic disease. AJNR Am J Neuroradiology 2012;33(8):1427–35.
[46] Li ML, Xu WH, Song L, et al. Atherosclerosis of middle cerebral artery: evaluation with high-resolution MR imaging at 3T. Atherosclerosis 2009;204(2):447–52.
[47] Xu WH, Li ML, Niu JW, et al. Intracranial artery atherosclerosis and lumen dilation in cerebral small-vessel diseases: a high-resolution MRI Study. CNS Neurosci Ther 2014;20(4):364–7.
[48] Zhou L, Li ML, Niu JW, et al. High-resolution MRI findings in patients with capsular warning syndrome. BMC Neurol 2014;14:16.
[49] Mazighi M, Labreuche J, Gongora-Rivera F, et al. Autopsy prevalence of intracranial atherosclerosis in patients with fatal stroke. Stroke 2008;39(4):1142–7.
[50] Chung GH, Kwak HS, Hwang SB, et al. High resolution MR imaging in patients with symptomatic middle cerebral artery stenosis. Eur J Radiol 2012;81(12):4069–74.
[51] Kim YJ, Lee DH, Kwon JY, et al. High resolution MRI difference between moyamoya disease and intracranial atherosclerosis. Eur J Neurol 2013;20(9):1311–8.
[52] Natori T, Sasaki M, Miyoshi M, et al. Evaluating middle cerebral artery atherosclerotic lesions in acute ischemic stroke using magnetic resonance T1-weighted 3-dimensional vessel wall imaging. J Stroke Cerebrovasc Dis 2014;23(4):706–11.
[53] Pfefferkorn T, Linn J, Habs M, et al. Black blood MRI in suspected large artery primary angiitis of the central nervous system. J Neuroimaging 2013;23(3):379–83.
[54] Swartz RH, Bhuta SS, Farb RI, et al. Intracranial arterial wall imaging using high-resolution 3-tesla contrast-enhanced MRI. Neurology 2009;72(7):627–34.
[55] Park JK, Lee CS, Sim KB, et al. Imaging of the walls of saccular cerebral aneurysms with double inversion recovery black-blood sequence. J Magn Reson Imaging 2009;30(5):1179–83.
[56] Portanova A, Hakakian N, Mikulis DJ, et al. Intracranial vasa vasorum: insights and implications for imaging. Radiology 2013;267(3):667–79.
[57] Qiao Y, Steinman DA, Qin Q, et al. Intracranial arterial wall imaging using three-dimensional high isotropic resolution black blood MRI at 3.0 Tesla. J Magn Reson Imaging 2011;34(1):22–30.
[58] Leng X, Wong KS, Liebeskind DS. Evaluating intracranial atherosclerosis rather than intracranial stenosis. Stroke 2014;45(2):645–51.
[59] Mathur K S, Kashyap S K, Kumar V. Correlation of the extent and severity of atherosclerosis in the coronary and cerebral arteries. Circulation 1963;27(5):929–34.
[60] Resch JA, Okabe N, Loewenson R, et al. A comparative study of cerebral atherosclerosis in a Japanese and Minnesota population. J Atheroscler Res 1967;7(5):687–93.
[61] Baker AB, Iannone A. Cerebrovascular disease. I. The large arteries of the circle of Willis. Neurology 1959;9(5):321.
[62] Bae HJ, Yoon BW, Kang DW, et al. Correlation of coronary and cerebral atherosclerosis: difference between extracranial and intracranial arteries. Cerebrovasc Dis 2006;21(1–2):112–9.
[63] Ritz K, Denswil NP, Stam OC, et al. Cause and mechanisms of intracranial atherosclerosis. Circulation 2014;130(16):1407–14.

[64] Maiellaro K, Taylor WR. The role of the adventitia in vascular inflammation. Cardiovasc Res 2007;75(4):640–8.
[65] Ritman EL, Lerman A. The dynamic vasa vasorum. Cardiovasc Res 2007;75(4):649–58.
[66] Kwon T-G, Lerman LO, Lerman A. The vasa vasorum in atherosclerosis: the vessel within the vascular wall. J Am Coll Cardiol 2015;65(23):2478–80.
[67] Dunmore BJ, McCarthy MJ, Naylor AR, et al. Carotid plaque instability and ischemic symptoms are linked to immaturity of microvessels within plaques. J Vasc Surg 2007;45(1):155–9.
[68] Yang WJ, Wong KS, Chen XY. Intracranial atherosclerosis: from microscopy to high-resolution magnetic resonance imaging. J Stroke 2017;19(3):249–60.
[69] Aydin F. Do human intracranial arteries lack vasa vasorum? A comparative immunohistochemical study of intracranial and systemic arteries. Acta Neuropathol 1998;96(1):22–8.
[70] Buckley ML, Ramji DP. The influence of dysfunctional signaling and lipid homeostasis in mediating the inflammatory responses during atherosclerosis. Biochim Biophys Acta 2015;1852(7):1498–510.
[71] Doherty TM, Asotra K, Fitzpatrick LA, et al. Calcification in atherosclerosis: bone biology and chronic inflammation at the arterial crossroads. Proc Natl Acad Sci U S A 2003;100(20):11201–6.
[72] Libby P. Molecular bases of the acute coronary syndromes. Circulation 1995;91(11):2844–50.
[73] Oppenheim C, Naggara O, Touzé E, et al. High-resolution MR imaging of the cervical arterial wall: what the radiologist needs to know. Radiographics 2009;29(5):1413–31.
[74] Chen XY, Wong KS, Lam WW, et al. Middle cerebral artery atherosclerosis: histological comparison between plaques associated with and not associated with infarct in a postmortem study. Cerebrovasc Dis 2008;25(1–2):74–80.
[75] Yuan C, Mitsumori LM, Ferguson MS, et al. In vivo accuracy of multispectral magnetic resonance imaging for identifying lipid-rich necrotic cores and intraplaque hemorrhage in advanced human carotid plaques. Circulation 2001;104(17):2051–6.
[76] Hatsukami TS, Ross R, Polissar NL, et al. Visualization of fibrous cap thickness and rupture in human atherosclerotic carotid plaque in vivo with high-resolution magnetic resonance imaging. Circulation 2000;102(9):959–64.
[77] Yuan C, Kerwin WS, Ferguson MS, et al. Contrast-enhanced high resolution MRI for atherosclerotic carotid artery tissue characterization. J Magn Reson Imaging 2002;15(1):62–7.
[78] Adams HP, Bendixen BH, Kappelle LJ, et al. Classification of subtype of acute ischemic stroke. Definitions for use in a multicenter clinical trial. TOAST. Trial of Org 10172 in Acute Stroke Treatment. Stroke 1993;24(1):35–41.
[79] Hart RG, Diener HC, Coutts SB, et al. Embolic strokes of undetermined source: the case for a new clinical construct. Lancet Neurol 2014;13(4):429–38.
[80] Bodle JD, Feldmann E, Swartz RH, et al. High-resolution magnetic resonance imaging: an emerging tool for evaluating intracranial arterial disease. Stroke 2013;44(1):287–92.
[81] Crisby M, Nordin-Fredriksson G, Shah PK, et al. Pravastatin treatment increases collagen content and decreases lipid content, inflammation, metalloproteinases, and cell death in human carotid plaques: implications for plaque stabilization. Circulation 2001;103(7):926–33.
[82] Lindenholz A, van der Kolk AG, Zwanenburg JJM, et al. The use and pitfalls of intracranial vessel wall imaging: how we do it. Radiology 2018;286(1):12–28.
[83] Zhang L, Zhang N, Wu J, et al. High resolution three dimensional intracranial arterial wall imaging at 3 T using T1 weighted SPACE. Magn Reson Imaging 2015;33(9):1026–34.
[84] Li ML, Xu YY, Hou B, et al. High-resolution intracranial vessel wall imaging using 3D CUBE T1 weighted sequence. Eur J Radiol 2016;85(4):803–7.
[85] Edelman RR, Chien D, Kim D. Fast selective black blood MR imaging. Radiology 1991;181(3):655–60.
[86] Li L, Miller KL, Jezzard P. DANTE-prepared pulse trains: a novel approach to motion-sensitized and motion-suppressed quantitative magnetic resonance imaging. Magn Reson Med 2012;68(5):1423–38.
[87] Fan Z, Sheehan J, Bi X, et al. 3D noncontrast MR angiography of the distal lower extremities using flow-sensitive dephasing (FSD)-prepared balanced SSFP. Magn Reson Med 2009;62(6):1523–32.
[88] Xie Y, Yang Q, Xie G, et al. Improved black-blood imaging using DANTE-SPACE for simultaneous carotid and intracranial vessel wall evaluation. Magn Reson Med 2016;75(6):2286–94.
[89] Wang J, Helle M, Zhou Z, et al. Joint blood and cerebrospinal fluid suppression for intracranial vessel wall MRI. Magn Reson Med 2016;75(2):831–8.
[90] Fan Z, Yang Q, Deng Z, et al. Whole-brain intracranial vessel wall imaging at 3 Tesla using cerebrospinal fluid-attenuated T1-weighted 3D turbo spin echo. Magn Reson Med 2017;77(3):1142–50.
[91] Yang H, Zhang X, Qin Q, et al. Improved cerebrospinal fluid suppression for intracranial vessel wall MRI. J Magn Reson Imaging 2016;44(3):665–72.
[92] Bouvy WH, Biessels GJ, Kuijf HJ, et al. Visualization of perivascular spaces and perforating arteries with 7 T magnetic resonance imaging. Invest Radiol 2014;49(5):307–13.
[93] Kleinloog R, Korkmaz E, Zwanenburg JJ, et al. Visualization of the aneurysm wall: a 7.0-tesla magnetic resonance imaging study. Neurosurgery 2014;75(6):614–22 [discussion: 622].
[94] Gutierrez J, Rosoklija G, Murray J, et al. A quantitative perspective to the study of brain arterial remodeling of donors with and without HIV in the Brain Arterial Remodeling Study (BARS). Front Physiol 2014;5:56.

[95] Jain KK. Some observations on the anatomy of the middle cerebral artery. Can J Surg 1964;7:134–9.
[96] Mandell DM, Mossa-Basha M, Qiao Y, et al. Intracranial vessel Wall MRI: principles and expert consensus recommendations of the American Society of Neuroradiology. AJNR Am J Neuroradiol 2017;38(2):218–29.
[97] Qiao Y, Zeiler SR, Mirbagheri S, et al. Intracranial plaque enhancement in patients with cerebrovascular events on high-spatial-resolution MR images. Radiology 2014;271(2):534–42.
[98] Antiga L, Wasserman BA, Steinman DA. On the overestimation of early wall thickening at the carotid bulb by black blood MRI, with implications for coronary and vulnerable plaque imaging. Magn Reson Med 2008;60(5):1020–8.
[99] Zhu C, Haraldsson H, Tian B, et al. High resolution imaging of the intracranial vessel wall at 3 and 7 T using 3D fast spin echo MRI. MAGMA 2016;29(3):559–70.
[100] Harteveld AA, van der Kolk AG, van der Worp HB, et al. High-resolution intracranial vessel wall MRI in an elderly asymptomatic population: comparison of 3T and 7T. Eur Radiol 2017;27(4):1585–95.
[101] Mossa-Basha M, Hwang WD, De Havenon A, et al. Multicontrast high-resolution vessel wall magnetic resonance imaging and its value in differentiating intracranial vasculopathic processes. Stroke 2015;46(6):1567–73.
[102] Andre JB, Bresnahan BW, Mossa-Basha M, et al. Toward quantifying the prevalence, severity, and cost associated with patient motion during clinical MR examinations. J Am Coll Radiol 2015;12(7):689–95.
[103] Bi X, et al. Motion-robust 3D Black-blood Carotid wall imaging using flow-sensitive dephasing preparation and stack-of-stars trajectory. In Proceedings of the ISMRM. 2015. Toronto, May 30 - June 5, 2015.
[104] Harteveld AA, Denswil NP, Siero JC, et al. Quantitative intracranial atherosclerotic plaque characterization at 7T MRI: an ex vivo study with histologic validation. AJNR Am J Neuroradiol 2016;37(5):802–10.
[105] Dieleman N, van der Kolk AG, Zwanenburg JJ, et al. Imaging intracranial vessel wall pathology with magnetic resonance imaging: current prospects and future directions. Circulation 2014;130(2):192–201.
[106] Alexander MD, Yuan C, Rutman A, et al. High-resolution intracranial vessel wall imaging: imaging beyond the lumen. J Neurol Neurosurg Psychiatry 2016;87(6):589–97.
[107] Turan TN, Bonilha L, Morgan PS, et al. Intraplaque hemorrhage in symptomatic intracranial atherosclerotic disease. J Neuroimaging 2011;21(2):e159–61.
[108] Mineyko A, Kirton A, Ng D, et al. Normal intracranial periarterial enhancement on pediatric brain MR imaging. Neuroradiology 2013;55(9):1161–9.
[109] den Hartog AG, Bovens SM, Koning W, et al. Current status of clinical magnetic resonance imaging for plaque characterisation in patients with carotid artery stenosis. Eur J Vasc Endovasc Surg 2013;45(1):7–21.
[110] Majidi S, Sein J, Watanabe M, et al. Intracranial-derived atherosclerosis assessment: an in vitro comparison between virtual histology by intravascular ultrasonography, 7T MRI, and histopathologic findings. AJNR Am J Neuroradiol 2013;34(12):2259–64.
[111] Chen X-Y, Lam WW, Ng HK, et al. Diagnostic accuracy of MRI for middle cerebral artery stenosis: a postmortem study. J Neuroimaging 2006;16(4):318–22.
[112] Chen XY, Wong KS, Lam WW, et al. High signal on T1 sequence of magnetic resonance imaging confirmed to be intraplaque haemorrhage by histology in middle cerebral artery. Int J Stroke 2014;9(4):E19.
[113] Turan TN, Rumboldt Z, Granholm AC, et al. Intracranial atherosclerosis: correlation between in-vivo 3T high resolution MRI and pathology. Atherosclerosis 2014;237(2):460–3.
[114] van der Kolk AG, Zwanenburg JJ, Denswil NP, et al. Imaging the intracranial atherosclerotic vessel wall using 7T MRI: initial comparison with histopathology. AJNR Am J Neuroradiol 2015;36(4):694–701.
[115] Klein IF, Lavallée PC, Touboul PJ, et al. In vivo middle cerebral artery plaque imaging by high-resolution MRI. Neurology 2006;67(2):327–9.
[116] Xu WH, Li ML, Gao S, et al. Middle cerebral artery intraplaque hemorrhage: prevalence and clinical relevance. Ann Neurol 2012;71(2):195–8.
[117] Jiang Y, Zhu C, Peng W, et al. Ex-vivo imaging and plaque type classification of intracranial atherosclerotic plaque using high resolution MRI. Atherosclerosis 2016;249:10–6.
[118] Wu XH, Chen XY, Fan YH, et al. High extent of intracranial carotid artery calcification is associated with downstream microemboli in stroke patients. J Stroke Cerebrovasc Dis 2017;26(2):442–7.
[119] Vakil P, Vranic J, Hurley MC, et al. T1 gadolinium enhancement of intracranial atherosclerotic plaques associated with symptomatic ischemic presentations. AJNR Am J Neuroradiol 2013;34(12):2252–8.
[120] Chaudhary V, Bano S. Imaging of the pituitary: recent advances. Indian J Endocrinol Metab 2011;15(Suppl 3):S216–23.
[121] Skarpathiotakis M, Mandell DM, Swartz RH, et al. Intracranial atherosclerotic plaque enhancement in patients with ischemic stroke. AJNR Am J Neuroradiol 2013;34(2):299–304.
[122] Kim JM, Jung KH, Sohn CH, et al. Middle cerebral artery plaque and prediction of the infarction pattern. Arch Neurol 2012;69(11):1470–5.
[123] Wu F, Song H, Ma Q, et al. Hyperintense plaque on intracranial vessel wall magnetic resonance imaging as

a predictor of artery-to-artery embolic infarction. Stroke 2018;49(4):905–11.
[124] Trivedi RA, U-King-Im JM, Graves MJ, et al. In vivo detection of macrophages in human carotid atheroma: temporal dependence of ultrasmall superparamagnetic particles of iron oxide-enhanced MRI. Stroke 2004; 35(7):1631–5.
[125] Hasan D, Chalouhi N, Jabbour P, et al. Early change in ferumoxytol-enhanced magnetic resonance imaging signal suggests unstable human cerebral aneurysm: a pilot study. Stroke 2012;43(12):3258–65.
[126] Liu Q, Huang J, Degnan AJ, et al. Comparison of high-resolution MRI with CT angiography and digital subtraction angiography for the evaluation of middle cerebral artery atherosclerotic steno-occlusive disease. Int J Cardiovasc Imaging 2013;29(7):1491–8.
[127] Bai X, Lv P, Liu K, et al. 3D black-blood luminal angiography derived from high-resolution MR vessel wall imaging in detecting MCA stenosis: a preliminary study. AJNR Am J Neuroradiol 2018;39(10):1827–32.
[128] Lee NJ, Chung MS, Jung SC, et al. Comparison of high-resolution MR imaging and digital subtraction angiography for the characterization and diagnosis of intracranial artery disease. AJNR Am J Neuroradiol 2016; 37(12):2245–50.
[129] Baik SH, Kwak HS, Hwang SB, et al. Three-dimensional black blood contrast enhanced magnetic resonance imaging in patients with acute ischemic stroke and negative susceptibility vessel sign. Eur J Radiol 2018;102: 188–94.
[130] Wang Y, Lou X, Li Y, et al. Imaging investigation of intracranial arterial dissecting aneurysms by using 3 T high-resolution MRI and DSA: from the interventional neuroradiologists' view. Acta Neurochir (Wien) 2014; 156(3):515–25.
[131] Tsukahara T, Minematsu K. Overview of spontaneous cervicocephalic arterial dissection in Japan. In: Laakso A, Hernesniemi J, Yonekawa Y, Tsukahara T, editors. Surgical management of cerebrovascular disease. Vienna (Austria): Springer Vienna; 2010. p. 35–40.
[132] Han M, Rim NJ, Lee JS, et al. Feasibility of high-resolution MR imaging for the diagnosis of intracranial vertebrobasilar artery dissection. Eur Radiol 2014; 24(12):3017–24.
[133] Gao PH, Yang L, Wang G, et al. Symptomatic unruptured isolated middle cerebral artery dissection: clinical and magnetic resonance imaging features. Clin Neuroradiol 2016;26(1):81–91.
[134] Kwak HS, Hwang SB, Chung GH, et al. High-resolution magnetic resonance imaging of symptomatic middle cerebral artery dissection. J Stroke Cerebrovasc Dis 2014; 23(3):550–3.
[135] Mizutani T. Natural course of intracranial arterial dissections. J Neurosurg 2011;114(4):1037–44.
[136] Arauz A, Márquez JM, Artigas C, et al. Recanalization of vertebral artery dissection. Stroke 2010;41(4):717–21.
[137] Xu WH, Li ML, Gao S, et al. In vivo high-resolution MR imaging of symptomatic and asymptomatic middle cerebral artery atherosclerotic stenosis. Atherosclerosis 2010;212(2):507–11.
[138] Tan TY, Kuo YL, Lin WC, et al. Effect of lipid-lowering therapy on the progression of intracranial arterial stenosis. J Neurol 2009;256(2):187–93.
[139] Obusez EC, Hui F, Hajj-Ali RA, et al. High-resolution MRI vessel wall imaging: spatial and temporal patterns of reversible cerebral vasoconstriction syndrome and central nervous system vasculitis. AJNR Am J Neuroradiol 2014;35(8):1527–32.
[140] Saam T, Habs M, Pollatos O, et al. High-resolution black-blood contrast-enhanced T1 weighted images for the diagnosis and follow-up of intracranial arteritis. Br J Radiol 2010;83(993):e182–4.
[141] Mandell Daniel M, Matouk CC, Farb RI, et al. Vessel wall MRI to differentiate between reversible cerebral vasoconstriction syndrome and central nervous system vasculitis. Stroke 2012;43(3):860–2.
[142] Scott RM, Smith ER. Moyamoya disease and moyamoya syndrome. N Engl J Med 2009;360(12):1226–37.
[143] Yuan M, Liu ZQ, Wang ZQ, et al. High-resolution MR imaging of the arterial wall in moyamoya disease. Neurosci Lett 2015;584:77–82.
[144] Ryoo S, Cha J, Kim SJ, et al. High-resolution magnetic resonance wall imaging findings of Moyamoya disease. Stroke 2014;45(8):2457–60.
[145] Matouk CC, Mandell DM, Günel M, et al. Vessel wall magnetic resonance imaging identifies the site of rupture in patients with multiple intracranial aneurysms: proof of principle. Neurosurgery 2013;72(3): 492–6 [discussion: 496].
[146] Horie N, Morikawa M, Fukuda S, et al. Detection of blood blister-like aneurysm and intramural hematoma with high-resolution magnetic resonance imaging. J Neurosurg 2011;115(6):1206–9.
[147] Edjlali M, Gentric JC, Régent-Rodriguez C, et al. Does aneurysmal wall enhancement on vessel wall MRI help to distinguish stable from unstable intracranial aneurysms? Stroke 2014;45(12):3704–6.
[148] Nagahata S, Nagahata M, Obara M, et al. Wall enhancement of the intracranial aneurysms revealed by magnetic resonance vessel wall imaging using three-dimensional turbo spin-echo sequence with motion-sensitized driven-equilibrium: a sign of ruptured aneurysm? Clin Neuroradiol 2016;26(3):277–83.
[149] Li B, Li H, Li J, et al. Relaxation enhanced compressed sensing three-dimensional black-blood vessel wall MR imaging: Preliminary studies. Magn Reson Imaging 2015;33(7):932–8.
[150] Busse RF, Brau AC, Vu A, et al. Effects of refocusing flip angle modulation and view ordering in 3D fast spin echo. Magn Reson Med 2008;60(3):640–9.